Electrochemical investigation of duplex stainless steel at carbon paste electrode and its application to the detection of dopamine, ascorbic and uric acid

R. Shashanka[1*], D. Chaira[1], B.E. Kumara Swamy[2]
[1]Department of Metallurgical and Materials Engineering, National Institute of Technology Rourkela-769008, India
[2]Department of P.G .Studies and Research in Industrial Chemistry, Kuvempu University, Jnana Sahyadri, Shankaraghatta 577451, Shimoga, Karnataka, India

Corresponding author:
***** E-mail address: shashankaic@gmail.com

Abstract— Nano-structured duplex stainless steel powders were synthesized by planetary milling of elemental Fe, Cr and Ni powders in dual-drive planetary mill for 10h. The prepared duplex stainless steel powders were characterized by X-ray diffraction, Scanning electron microscope, High resolution transmission microscope, BET surface area measurement. The electrochemical property of prepared duplex stainless steel powder was investigated by cyclic voltammetry. Nano structured duplex stainless steel modified carbon paste electrode shows an excellent sensitivity towards the oxidation of dopamine, ascorbic acid and uric acid in 0.2M phosphate buffer at 7.2 pH. Electrocatalytic property of analyte was investigated at 2, 4, 6 and 8mg concentrations of modifier. The 4mg duplex modified carbon paste electrode show maximum anodic peak current of 25.61μA and hence it is used as modifier to study the electrochemical properties of dopamine, ascorbic acid and uric acid. The fabricated electrode exhibits fast, stable sensitivity, reliable and resistant to material fouling.

Index Terms— Duplex stainless steel, cyclic voltammetry, dopamine, ascorbic acid, uric acid, carbon paste, modifier.

1 INTRODUCTION

Now a day electrochemists are putting efforts to develop voltammetric methods for the determination of bioactive materials like dopamine (DA), ascorbic acid (AA) and uric acid (UA) [1]. DA is a medication type of a substance naturally present in body and it improves not only the pumping potential of heart but also the flow of blood to kidneys. It is used to treat low blood pressure, heart attacks, trauma, heart failure, kidney failure and other serious medical conditions. It acts as a neurotransmitter and controls various physiological events such as function of renal, cardiovascular, hormonal and nervous systems. Deficiency of DA causes neurological diseases such as Parkinson's disease [2], Alzheimer's disease [3] and schizophrenia [4]. Therefore it is very important to measure the DA concentration in biological body fluids. Hence we developed selective and sensitive electrochemical method for the determination of DA concentration by cyclic voltammetry.
Chandrashekar et al. reported the determination of DA by polyethylene glycol modified carbon paste electrode. They reported the effect of scan rate, concentration of DA on anodic peak current [5]. Manjunatha et al. investigated the electrochemical response of DA using Poly (tannic acid). They reported the effect of pH, concentration and potential sweep rate on the anodic peak potential of DA [6].
Ascorbic acid is also a naturally occurring antioxidant present in higher concentrations along with low concentration DA. It is commonly known as vitamin C and is one of the very significant vitamins broadly existing in many plants. It involves some important biological applications such as free radical scavenging, cancer prevention and improves the immunity. The wide source of AA is food, plant and animal tissues. Recommended daily intake of AA is about 70–90 mg [7]. The deficiency of AA causes scurvy, gingival bleeding; and its excessive intake leads to urinary stone, diarrhoea and stomach convulsion [8]. The intravenous high dosage of AA is used as chemotherapeutic and biological response modifying agent [9]. Therefore, it is very important to measure the concentration of AA in aqueous solutions. Lin et al. successfully determined AA by using Poly (xanthurenic acid) and multi-walled carbon nanotubes hybrid composites. This hybrid composite show appreciable stability in various scan rates and different pH conditions [7]. Florou et al. electrochemically determined the AA using 2, 6-dichlora-phenol indo phenol cellulose acetate polymeric film modified electrode. They studied the operational stability of AA sensor by continuous exposure to the flow stream [10].
Uric acid (2, 6, 8–trihydroxypurine) is one of the major nitrogenous compound present in urine. It is produced in human body due to the metabolic activity of purine. Its higher levels in the blood (hyper uricemia or Lesch-Nyhan syndrome) lead to disorders like gout, kidney and cardiac problems [11]. Shashanka et al. studied the electrochemical response of UA using silver nanoparticles modified carbon paste electrode. They studied the effect of scan rate, concentration of analyte and modifier on the anodic peak current [12].
All these bioactive compounds more often exist together at biological system and exhibits very close oxidation potential resulting in overlapping voltammetric response. Therefore, it is difficult to determine DA, AA and UA concentration simultaneously. Hence, we studied the electrochemical behaviour of

International Journal of Scientific & Engineering Research, Volume 6, Issue 9, September-2015
ISSN 2229-5518

above compounds individually using nano structured duplex stainless steel powder as a modified carbon paste electrode.
Nano structured duplex stainless steel powder was synthesized by milling elemental composition of Fe (99.5% pure), Cr (99.8% pure) and Ni (99.5% pure) powders in a specially designed dual drive planetary mill (DDPM). Although many research papers are available in determining the cyclic voltammetric response of DA, AA and UA by using different types of surfactants, dyes and polymers; but no one reported the use of nano structured duplex stainless steel powder as modifier to study the electrochemical oxidation of DA, AA and UA. Duplex modified carbon paste electrode (DMCPE) show improved electro catalysis, resistant to surface fouling and undesired electrode reactions. Hence, DMCPE is found to be a suitable sensor for the determination of DA, AA and UA.

2 EXPERIMENTAL

2.1 Reagents and chemicals

Elemental powder mixture of Fe (99.5% pure), Cr (99.8% pure) and Ni (99.5% pure) were purchased from Loba chemicals. Dopamine, perchloric acid, Hydrogen peroxide, sodium dihydrogen orthophosphate dehydrate and di-sodium hydrogen phosphate anhydrous of analytical grade quality were purchased from sd. Fine chemicals. All the above reagent solutions were prepared by dissolving in double distilled water. Graphite powder was purchased from Merck chemicals.

2.2 Apparatus

Milling of the duplex composition (Fe-18Cr-13Ni) was carried out in a specially designed DDPM. The electrochemical experiments were performed by using electrochemical work station CHI-660c model. All the experiments were carried out in a conventional three electrode system consist of working electrode (carbon paste electrode of 3mm diameter), platinum wire as counter electrode and Ag/AgCl saturated KCl electrode as reference electrode. The microstructure of duplex stainless steel and modified electrodes were carried out using Scanning electron microscopy (SEM) of JEOL JSM-6480LV model. X-ray diffraction (XRD) studies were performed in PAN analytical Xpert Pro XRD. TEM studies of the milled duplex stainless steel powders were carried out using JEOL JEM-2100. Quantachrome/AUTOSORB-1 model was used to measure the surface area of the duplex stainless steel powder. The pH of buffer solutions was measured with digital pH meter MK VI.

2.3 Synthesis of Duplex stainless steel powders by DDPM

Elemental Fe, Cr and Ni powder mixtures were used as starting materials and their composition Fe-18Cr-13Ni was selected from Schaeffler diagram. The above composition was milled in DDPM for 10h with ball-to-powder weight ratio of 6:1. The milling media consist of 1kg stainless steel balls of 8mm diameter. The angular velocity of the vial and the supporting main shaft were maintained at 620 and 275 rpm respectively. The entire milling experiment was carried out under toluene atmosphere to prevent oxidation. The details of milling parameters, mill fabrication and synthesis of Fe-18Cr-13Ni were reported by the authors in their previous publications [13-15].

2.4 Fabrication of the carbon paste electrode

. The carbon paste electrode (CPE) was prepared by hand-mixing of graphite powder and silicon oil at a ratio 70:30 by wt. in an agate mortar. The homogeneous carbon paste electrode was packed into a cavity of homemade carbon paste electrode of diameter 3 mm. The DMCPE was prepared by hand mixing of 2, 4, 6 and 8mg duplex stainless steel powder individually with graphite powder and silicon oil. The electrode surface was smoothed by rubbing slowly on a piece of weighing paper. The electrical contact was supplied by copper wire connected to the paste at the tube end.

3 Results and discussion

3.1 X-Ray Diffraction study

The XRD spectrum of Fe-18Cr-13Ni (duplex composition) at 0h (Before milling) and 10h (After milling) is shown in Fig. 1. Before milling, the elemental powder mixture depicts sharp crystalline diffraction peaks. Bu after 10h of milling duplex stainless steel powder shows broad diffraction peaks due to the refined grain size, increased defects and strain. During milling, Cr and Ni atoms diffuse in to the Fe lattice and forms solid solution by micro segregating at grain boundaries. Duplex stainless steel powder composition exhibits both austenite and ferrite phases as shown in the XRD spectra. Lattice parameter of 0 and 10h duplex stainless steel is calculated by using Nelson-Riley method [16] and is found to be 3.05Å and 3.56Å respectively. The lattice parameter value increases from 0 to 10h due to the interstitial diffusion of Cr and Ni atoms in to Fe lattice. Duplex stainless steel undergoes many phenomenons like grain size reduction, structural defect and amorphization during milling. This increases the volume fraction of grain boundaries especially at point and linear defects. The refinement of grain size to nano level increases the volume fraction further and this result in more defect storage sites and shorter diffusion paths [13].

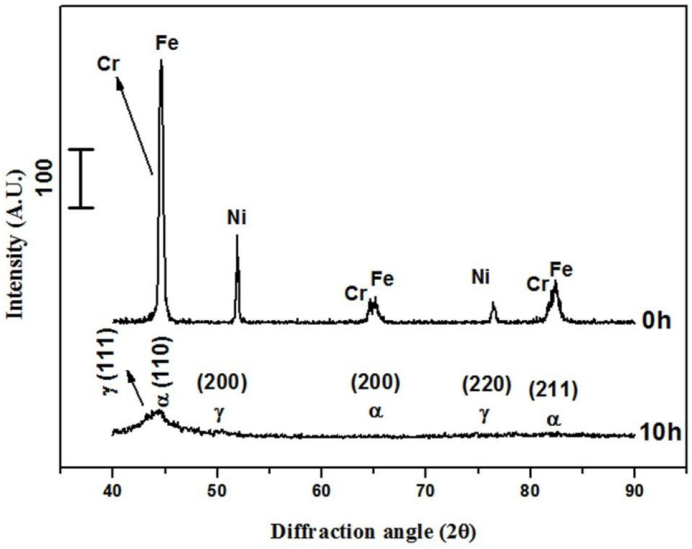

Fig. 1 XRD spectrum of Fe-18Cr-13Ni (duplex stainless steel composition) milled for 0h and 10h respectively

International Journal of Scientific & Engineering Research, Volume 6, Issue 9, September-2015
ISSN 2229-5518

3.2 Microstructure study

3.2.1 Scanning electron microscopy (SEM)

The microstructure of duplex stainless steel powder is studied successfully by SEM. Fig. 2 (a) and 2 (b) shows the SEM micrographs of duplex stainless steel powder milled for 0h and 10h respectively. At the beginning the powder particle are bulky and random in size but as milling starts elemental particles forms plate like morphology due to ductile nature of iron. Finally ductile particles undergo work hardening, material transfer and micro segregation at grain boundaries to form extended solid solution. This results in very fine, regular, uniform and spherical duplex stainless steel powder particles. Fig. 2 (c) and 2 (d) depict the SEM images of BCPE and DMCPE. From the topographic study it is observed that the surface of BCPE is irregular with flakes of graphite, whereas the surface of DMCPE is flat and regular with graphite flakes. This difference in surface topography also plays an important role in transfer of electrons. Quantitative and qualitative analysis is carried out using EDX spectrum to confirm the elemental composition of duplex stainless steel powder. Fig. 2 (e) shows a standard EDX spectrum of 10h milled duplex stainless steel powder sample. From the spectrum it is confirmed that chemical composition of 10h milled duplex stainless steel is almost same as parental powder composition.

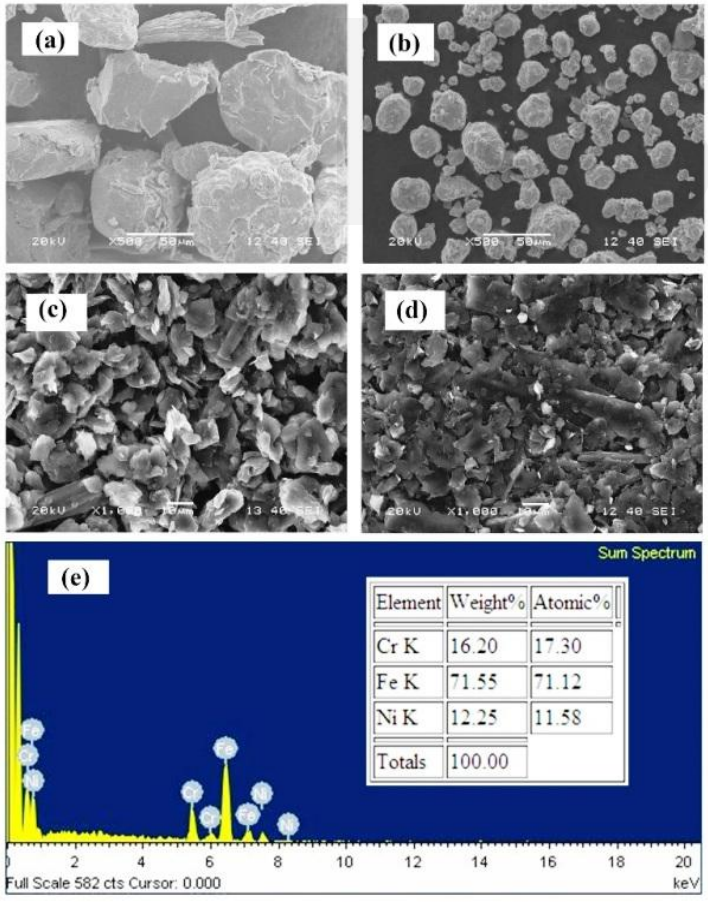

3.2.2 High resolution transmission electron microscopy (HRTEM)

The diffraction pattern, lattice spacing and microstructure of 10h milled duplex stainless steel powder samples are studied by HRTEM. Fig. 3 (a), 3 (b) and 3 (c) show the bright field TEM micrographs, SAED patterns and lattice images of 10h milled duplex stainless steel powder respectively.

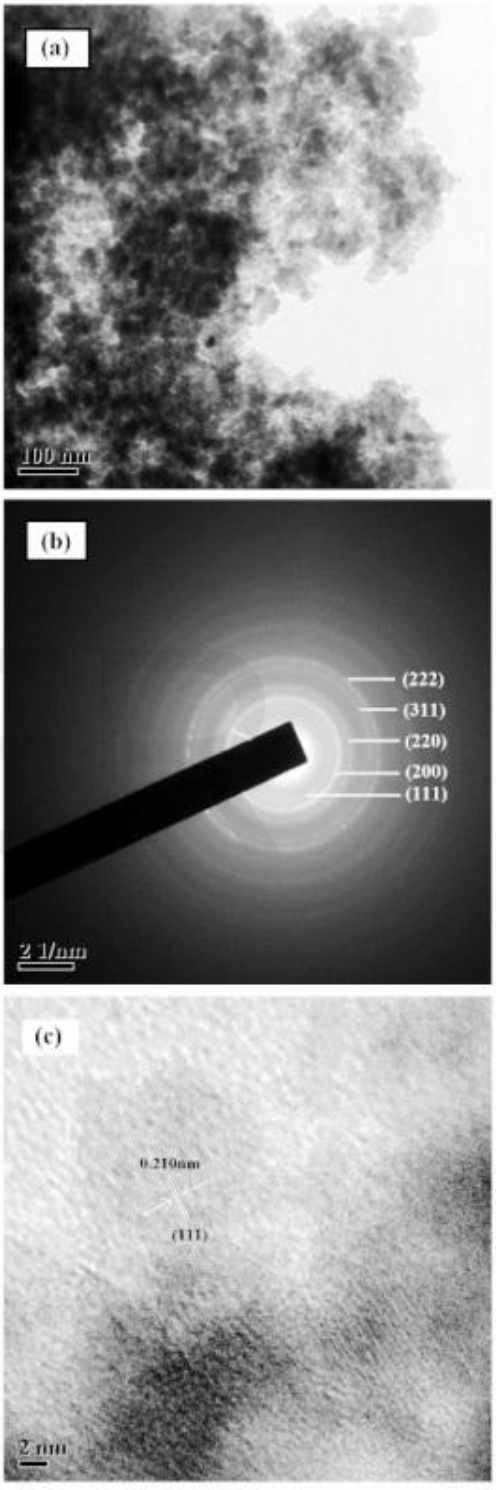

Fig. 3 TEM images of duplex stainless steel powder (a) TEM image (b) SAED pattern (c) HRTEM to measure lattice spacing

International Journal of Scientific & Engineering Research, Volume 6, Issue 9, September-2015
ISSN 2229-5518

Fig. 3 (a) shows bright field image of duplex stainless steel crystallites with an average size around 20nm each. Due to nano size and high surface area and high surface energy the particles agglomerates easily. Different crystallographic planes are indexed using SAED ring pattern as shown in the Fig 3 (b) and it confirms the FCC structure of duplex. The SAED pattern contains airy ring structures with few spotty appearances, which confirms the formation of nano-structured duplex stainless steel powder. Fig. 3 (c) shows lattice spacing of austenite (111) plane and it is found to be 2.105Å.

3.3 BET surface area measurement

Usually nano particles have a large surface area due to very fine size. The specific surface area is measured using the nitrogen gas adsorption technique developed by Brunauer, Emmett, and Teller, commonly known as the BET method [17]. BET surface area measurement mainly based upon simplified adsorption gas model, solid surface and on pore structure [18]. Nitrogen gas adsorb on particles in the form of multi layers, in which volume adsorbed is a summation of the adsorbed volumes of each layer [19].

BET surface area can also be calculated by using following equation [19]

$$\frac{P/P_0}{S(1-P/P_0)} = \frac{1}{V_m C} + \frac{C-1}{V_m C}\frac{P}{P_0} \quad (1)$$

Where, P is the equilibrium pressure, P_0 is the saturated vapour pressure of nitrogen, V is the amount of gas forming a monolayer on the solid surface (monolayer capacity) and C is a constant related to the heat of adsorption in the first layer. A plot of $(P/P_0) / S(1-P/P_0)$ versus P/P_0 gives a straight line from which the monolayer capacity V_m can be evaluated. From the obtained V_m value, the BET specific surface area can be calculated using the cross-sectional area.

Quantachrome / AUTOSORB-1 model is used to measure the total surface area of the DDPM milled 0h and 10h duplex stainless steel powder samples by standard volumetric nitrogen adsorption method at 77 K. Fig. 4 (a) and 4 (b) shows the adsorption–desorption isotherm of nano structured duplex stainless steel powders milled for 0 and 10h respectively. The BET surface area and total pore volume of 0h milled duplex stainless steel powder is found to be 7.65m^2/g and 0.109g/cc respectively. Similarly 10h milled duplex stainless steel powder is found to be 39.26m^2/g and 0.598g/cc respectively. Before milling, surface area and pore volumes are very less and they start to increase with milling. This is due to the increased volume fraction, amorphization, plastic deformation and refinement of size.

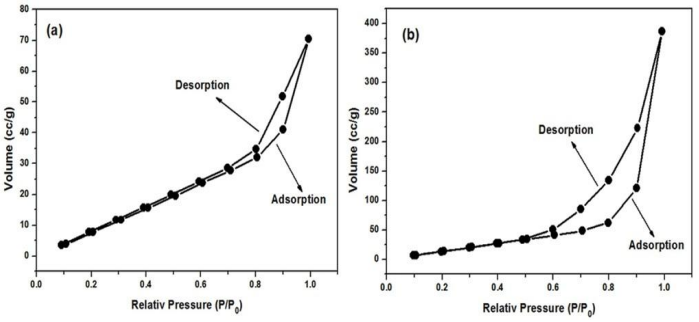

Fig. 4 Adsorption-Desorption curves of duplex stainless steel powder milled for (a) 0h (b) 10h respectively

3.4 Electro catalytic response of DA at DMCPE

3.4.1 Concentration variation of nano structured duplex stainless steel powder

The effect of different concentrations of modifier is studied and it is one of the most important parameter which decides the efficiency of the electrode performance as a sensor. In the present work, we used nanostructured duplex stainless steel powder as a modifier to study the electrochemical behaviour of DA, AA and UA effectively. The concentration of duplex stainless steel is varied from 2 to 8mg to investigate the electro catalytic behaviour of 2mM DA in 0.2M phosphate buffer (pH 7.2) at sweep potential from -200 to 600mV and scan rate of 100mVs^{-1}. Among 2, 4, 6 and 8mg concentration of DMCPE, 4mg DMCPE had shown maximum anodic peak current of 25.61µA. Fig. 5 (a) shows a plot of variation of anodic peak currents with different concentration of duplex stainless steel. From the plot it is clear that anodic peak current increases with modifier concentration up to 4mg and then decreases with further increase in the concentration. This is due to the resultant decrease in actual electrode area and reduced number of oxidation sites in the electrode surface [20]. Hence main role of a modifier is to enhance the peak current and decrease the over potential for the oxidation and reduction of DA. Duplex stainless steel satisfies the above condition and hence used as a modifier in the present work. Fig. 5 (b) shows the cyclic voltammogram of bare carbon paste electrode (BCPE) and 4mg DMCPE. The dotted curve and straight line curve voltammograms represent the 2Mm DA at BCPE and DMCPE respectively. The anodic peak current of BCPE is 13.95µA and that of DMCPE is 25.61µA. Hence 4mg DMCPE is selected as the modifier for the further determination of DA, AA and UA.

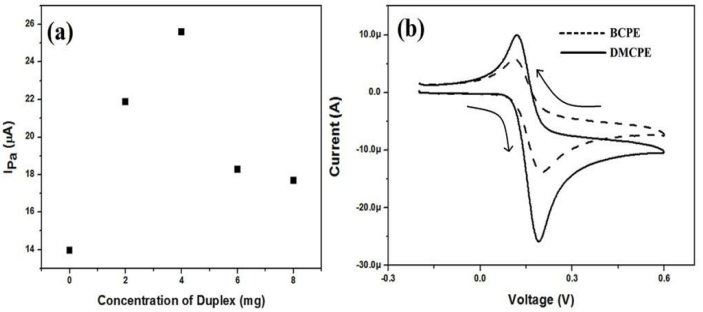

Fig. 5 (a) Plot of anodic peak currents with different concentration of duplex stainless steel in 2mM DA (b) Cyclic voltammogram of bare carbon paste electrode (BCPE) and 4mg DMCPE in 2mM DA at 100mVs^{-1} and in PBS of pH 7.2

International Journal of Scientific & Engineering Research, Volume 6, Issue 9, September-2015
ISSN 2229-5518

3.4.2 Effect of scan rate

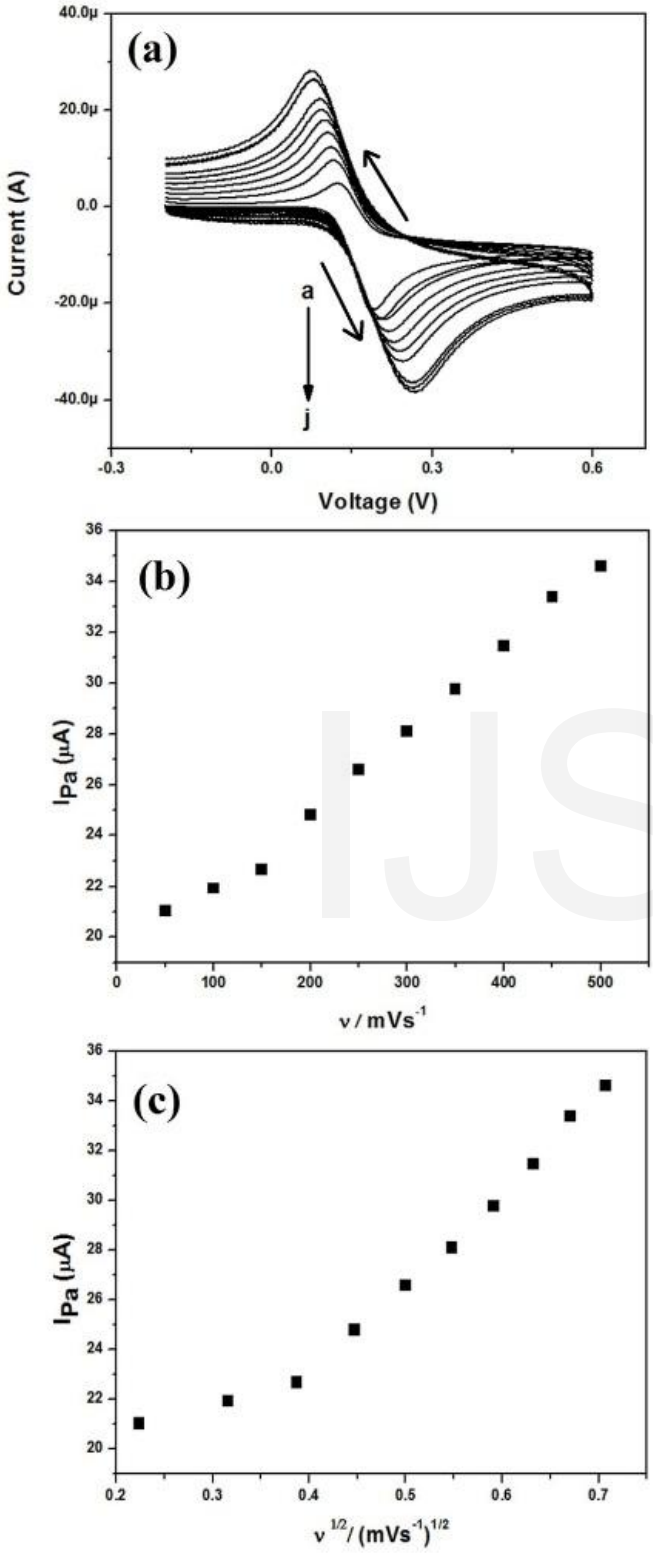

Fig. 6 (a) Cyclic voltammogram of 2mM DA at 50 to 500mVs^{-1} scan rate (a=50, b=100, ..., j=500mVs^{-1}) in PBS of pH 7.2 (b) Plot of anodic peak current vs scan rate (c) Plot of anodic peak current vs. square root of scan rate

Scan rate is an important parameter to study the kinetics of the electrode reaction and it is performed by increasing the scan rate from 50 to 500mVs^{-1} for 2mM DA in phosphate buffer solution (PBS) of pH 7.2. Fig. 6 (a) shows the voltammogram of DA at 4mg DMCPE. From the figure it is clear that, increase in scan rate from 50 to 500mVs^{-1} increases the anodic and cathodic peak current of DA due to the direct electron transfer between DA and the modified electrode surface. The potential difference between anodic and cathodic peak potentials also increases with increase in scan rate [21, 22]. Fig. 6 (b) shows the plot of anodic peak current vs. scan rate; their correlation coefficient is found to be 0.9924. Similarly Fig. 6 (c) depicts the plot of anodic peak current vs. square root of scan rate and its correlation coefficient is 0.9488. Hence all the electrode process is found to be adsorption controlled [6].

3.4.3 Effect of Dopamine concentration

Generally, anodic peak current increases with increase in the concentration of DA. Electrochemical response of DA at 2 to 3mM concentration is studied by using 4mg DMCPE. The voltammogram of different concentration of DA is shown in the fig. 7 (a). From the figure it is clear that increase in DA concentration increases the anodic peak current. Fig. 7 (b) shows the plot of anodic peak current vs. different concentration of DA. Plot depicts the linear relationship between peak current and concentration of DA with correlation coefficient of 0.9614. Anodic peak current at 2 and 2.1mM DA concentration show linear relationship but from 2.1 to 2.3mM there is no much increase in current and from 2.3 to 3mM DA concentration, the current increases linearly as shown in the plot. The anodic peak current at 2mM DA is 15.51μA and at 3mM DA concentration is increased to 19.10μA.

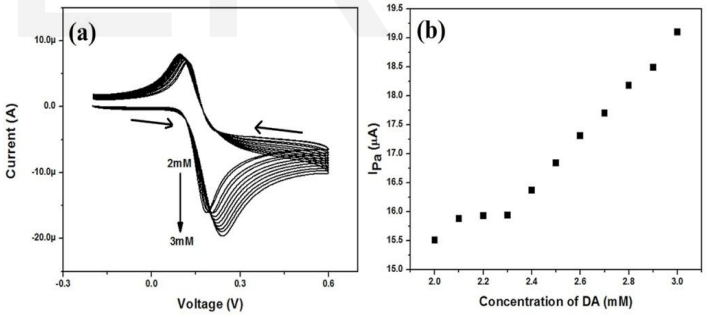

Fig. 7 (a) Cyclic voltammogram of 2 to 3mM concentration of DA at 100mVs^{-1} in PBS of pH 7.2 (b) Plot of anodic peak current vs. different concentration of DA

3.4.4 Effect of pH

The effect of pH variation on the peak potential of DA is studied successfully using 4mg DMCPE at 0.2M phosphate buffer solution with scan rate of 100mVs^{-1}. The anodic peak potential of 2mM DA is measured at different pH from 5.7 to 8. The voltammogram of different pH is shown in fig. 8 (a). From the figure it is clear that, both anodic and cathodic peak potentials of DA are shifted to a lower potential side with increase in pH. This is due to the increased rate of DA oxidation at higher pH. The graph shows good linearity and it obeys the Nernst Equation for equal number of electron and proton transfer reactions [23]. Fig. 8 (b) represents the plot of pH vs. anodic peak potential of DA. Anodic peak potential gradually decreases from

International Journal of Scientific & Engineering Research, Volume 6, Issue 9, September-2015
ISSN 2229-5518

pH 5.7 to 8 with correlation coefficient of 0.9574. At pH 5.7 the oxidation peak potential is 309mV and at pH 8 it is decreased to 190mV as shown in the plot.

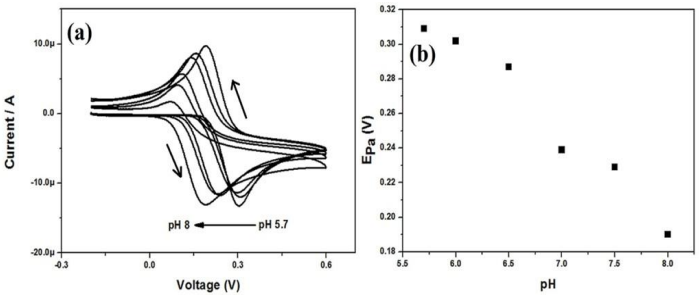

Fig. 8 (a) Cyclic voltammogram of 2mM DA at different pH of PBS buffer solutions at 100mVs^{-1} (b) Plot of anodic peak current vs. different pH from values 5.7 to 8

3.5 Electro catalytic response of AA at DMCPE

It is very difficult to measure the electrochemical response of AA in presence of electro active compounds like DA because DA can interfere the measurement of biochemical parameters by oxidising at same potential of AA and leads to wrong results [24-26]. Fig. 9 demonstrates the cyclic voltammogram of DMCPE and BCPE at a scan rate of 100mVs^{-1} and 2mM AA in phosphate buffer of pH 7.2. BCPE shows the anodic peak current of 100.90µA; whereas 4mg DMCPE shows anodic peak current of 143.52µA. From the voltammogram it is clear that DMCPE shows a better catalytic activity towards AA. Therefore oxidation potential is shifted towards negative side due to the fast electron transfer during oxidation [27]. The dotted and straight line curves in the voltammogram represent BCPE and DMCPE respectively at 2Mm AA.

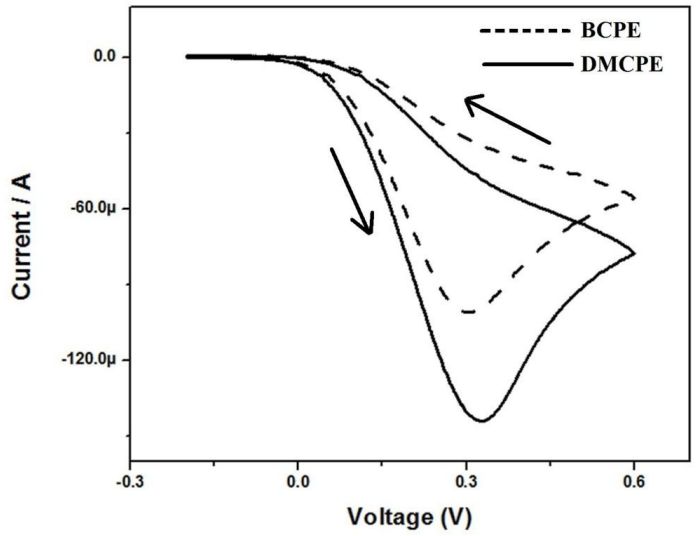

Fig. 9 Cyclic voltammogram of bare carbon paste electrode (BCPE) and 4mg DMCPE in 2mM AA at 100mVs^{-1} and in PBS of pH 7.2

3.5.1 Effect of scan rate

Electrochemical response of 2mM AA is performed by varying the scan rate from 50 to 300mVs^{-1} in PBS of pH 7.2. Fig. 10 (a) shows the voltammogram 2Mm AA at different scan rates. Anodic peak current and peak potential goes on increasing with increase in scan rate as shown in the figure. Fig. 10 (b) depicts the plot of scan rate vs. anodic peak current of AA at 100mVs^{-1} and the peak current varies from 76.8µA at 50mVs^{-1} to 110.65µA at 300mVs^{-1}. The correlation coefficient is found to be 0.9123 and this reveals that electrode process is adsorption controlled. Similarly, fig. 10 (c) represents the plot of square root of scan rate vs. anodic peak current of 2mM AA and their correlation coefficient is found to be 0.9473.

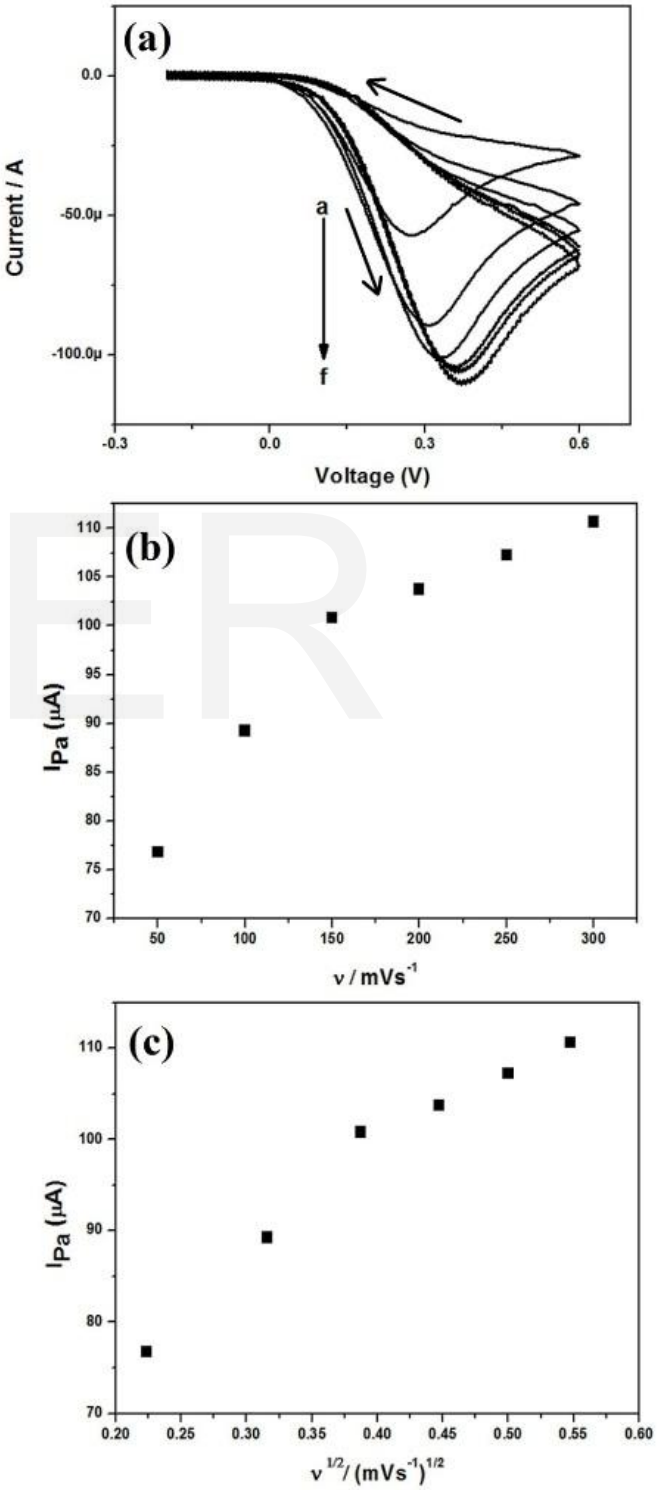

Fig. 10 (a) Cyclic voltammogram of 2mM AA at 50 to 300mVs^{-1} scan rate

International Journal of Scientific & Engineering Research, Volume 6, Issue 9, September-2015
ISSN 2229-5518

(a=50, b=100, ..., f=300mVs^{-1}) in PBS of pH 7.2 (b) Plot of anodic peak current vs. scan rate (c) Plot of anodic peak current vs. square root of scan rate

3.5.2 Effect of Ascorbic acid concentration

As the concentration of AA in an electrochemical cell increases from 2mM to 2.6mM; oxidation peak current also increases linearly. The voltammogram of different concentrations of AA is shown in fig. 11 (a). The anodic peak current increases from 63.52µA to 103.36µA at 2mM to 2.6mM AA concentration respectively. More voltage is required to oxidise the AA at higher concentrations; therefore anodic peak potential shift towards maximum values at higher concentrations. Oxidation potential increases from 309 to 371mV with increase in concentration of AA from 2mM to 2.6mM respectively. Fig. 11 (b) depicts the plot of anodic peak current vs. different concentration of AA and it shows linear relationship with correlation coefficient of 0.9790.

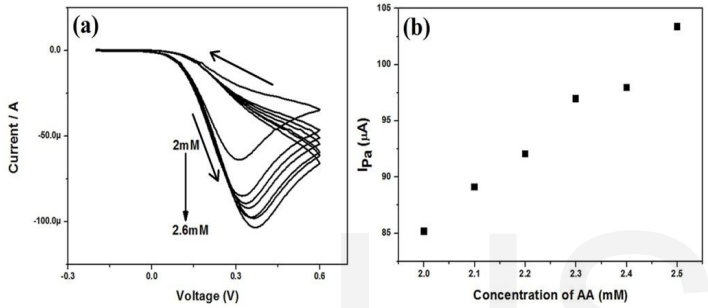

Fig. 11 (a) Cyclic voltammogram of 2 to 2.6mM concentration of AA at 100mVs^{-1} in PBS of pH 7.2 (b) Plot of anodic peak current vs. different concentration of AA

3.5.3 Effect of pH

Emphatically pH plays an important role in redox potential of almost all the analyte. Hence we studied the effect of different pH on the peak potential of AA using 4mg DMCPE. The oxidation peak potential of 2mM AA is measured at different pH from 5.7 to 8 at a scan rate of 100mVs^{-1}. Fig 12 (a) represents the voltammogram of AA at different pH solutions. From the figure it is clear that, both anodic and cathodic peak potentials of AA are shifted towards a lower potential side with increase in pH. This is due to the increased oxidation rate of AA at higher pH. Fig. 12 (b) represents the plot of pH vs. anodic peak potential of AA. Anodic peak potential decreases from pH 5.7 to 8 with correlation coefficient of 0.9875 as shown in the plot. At pH 5.7 the oxidation peak potential is 350mV and at pH 8 it is decreased to 322mV.

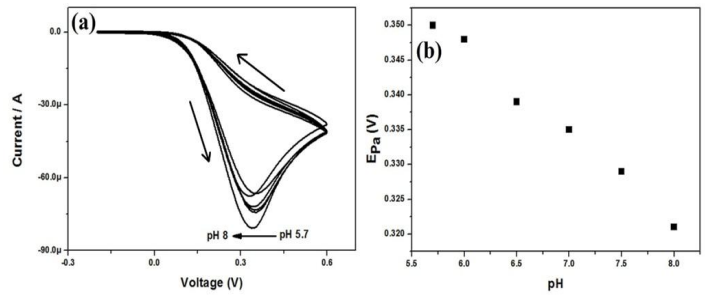

Fig. 12 (a) Cyclic voltammogram of 2mM AA at different pH of PBS buffer solutions at 100mVs^{-1} (b) Plot of anodic peak current vs. different pH from values 5.7 to 8

3.6 Electro catalytic response of UA at DMCPE

Fig. 13 shows the cyclic voltammogram of 2mM UA at BCPE and DMCPE in PBS (pH 7.2). The anodic peak current of BCPE is found to be 14.34µA and that of DMCPE is 19.36µA and there is very negligible shift of anodic peak potential towards positive side. The dotted curve and a straight line curve of voltammogram represent the oxidation peak of BCPE and DMCPE respectively. There is a considerable difference in anodic peak current between BCPE and DMCPE and hence one can easily resolve them. Therefore, 4mg DMCPE acts as a better electrochemical sensor for detecting UA.

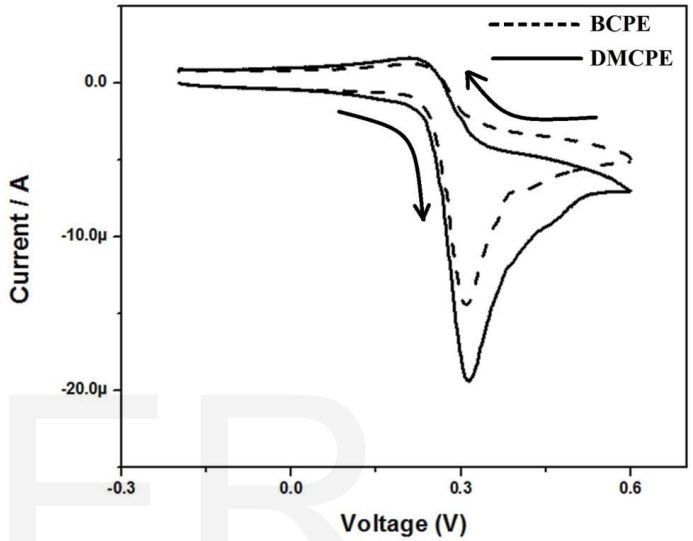

Fig. 13 Cyclic voltammogram of bare carbon paste electrode (BCPE) and 4mg DMCPE in 2mM UA at 100mVs^{-1} and in PBS of pH 7.2

3.6.1 Effect of scan rate

Fig. 14 (a) shows the voltammogram of 2mM UA at scan rate of 50 to 300mVs^{-1} in PBS of pH 7.2. Anodic peak current and peak potential goes on increasing with increase in the scan rate but cathodic peak current and potential show very negligible shift as shown in the figure. Fig 14 (b) represents the plot of scan rate vs. anodic peak current of UA at 100mVs^{-1} in PBS of pH 7.2 and the anodic peak current varies from 10.08 to 16.90µA at a scan rate of 50 to 300mVs^{-1}. The correlation coefficient is found to be 0.9560 and this reveals that electrode process is adsorption controlled. Similarly plot of square root of scan rate vs. anodic peak current of 2mM UA is shown in fig. 14 (c) and their correlation coefficient is found to be 0.9345.

International Journal of Scientific & Engineering Research, Volume 6, Issue 9, September-2015
ISSN 2229-5518

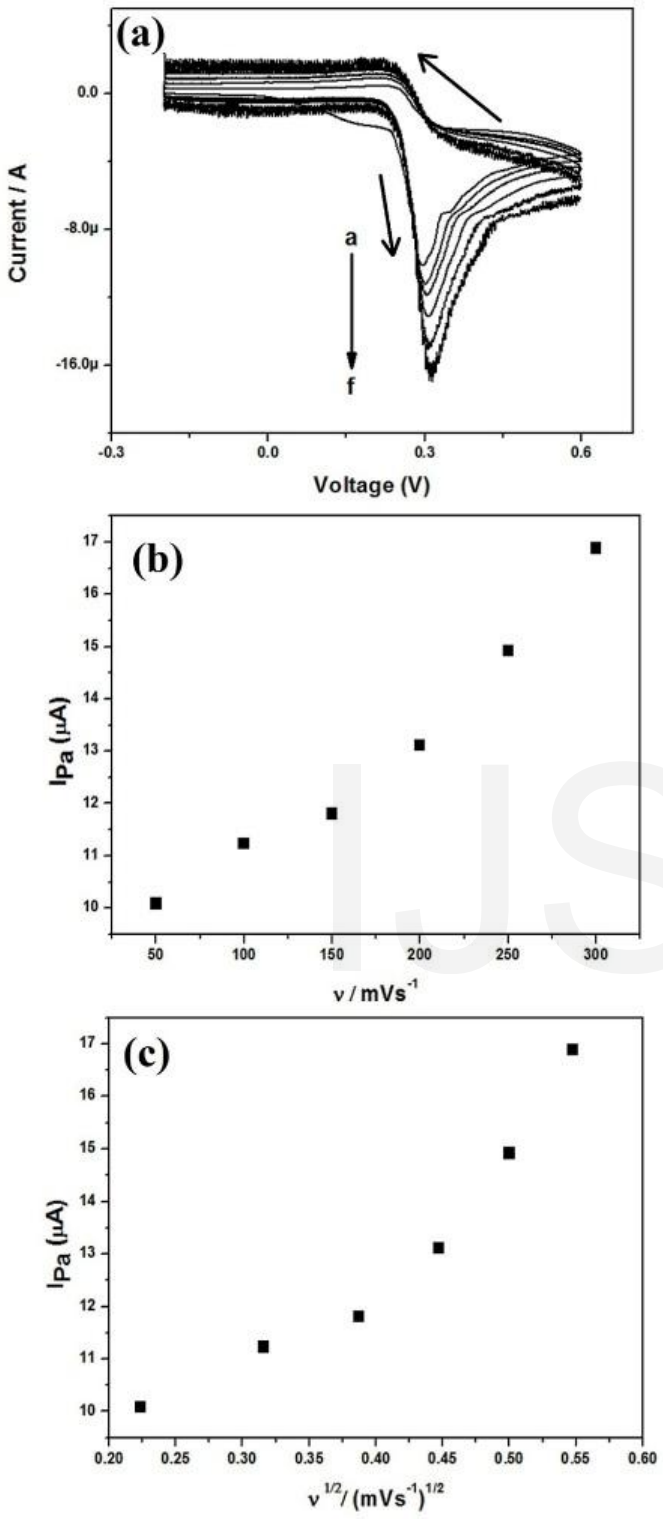

Fig. 14 (a) Cyclic voltammogram of 2mM UA at 50 to 300mVs^{-1} scan rate (a=50, b=100, ..., f=300mVs^{-1}) in PBS of pH 7.2 (b) Plot of anodic peak current vs. scan rate (c) Plot of anodic peak current vs. square root of scan rate

3.6.2 Effect of Concentration of Uric acid

The voltammogram of different concentrations of UA (2mM to 2.6mM) in PBS buffer of pH 7.2 is shown in fig. 15 (a). From the voltammogram it is clear that the oxidation peak current increases linearly with increase in the concentration of UA. The anodic peak current increases from 9.90μA to 15.12μA at 2mM to 2.6mM UA respectively. Here anodic peak potential shifts slightly towards the higher potential value with increase in the concentration of UA. The oxidation peak potential at 2 and 2.6mM UA concentrations is measured to be 301mV and 316mV respectively. There is no shift of either cathodic peak current or cathodic peak potential of 2mM UA. Fig. 15 (b) represents the plot of anodic peak current vs. different concentrations of UA and it shows a linear relationship with correlation coefficient of 0.9780.

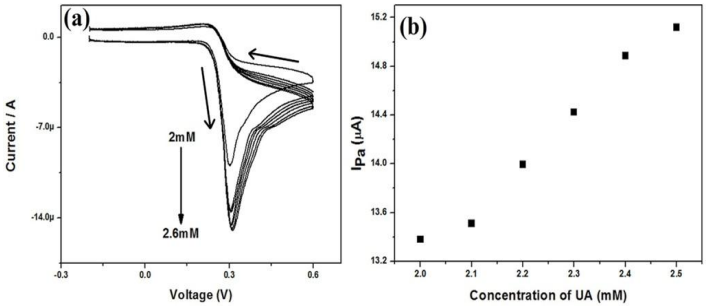

Fig. 15 (a) Cyclic voltammogram of 2 to 2.6mM concentration of UA at 100mVs^{-1} in PBS of pH 7.2 (b) Plot of anodic peak current vs. different concentration of UA

3.6.3 Effect of pH

Fig. 16 (a) represents the voltammogram of 2mM UA measured at different pH from 5.7 to 8. Both anodic and cathodic peak potentials of 2mM UA shift towards the lower potential side due to the increased redox rate of UA at higher pH. The anodic peak current decreases with increase in the pH value as shown in the figure. Fig. 16 (b) represents the plot of different pH vs. anodic peak potential of UA. The anodic peak potential of 2mM UA at pH 5.7 is 381mV and at pH 8 is 305mV. The plot shows the linear decrease in the anodic peak potential from pH 5.7 to 8 with correlation coefficient of 0.9560.

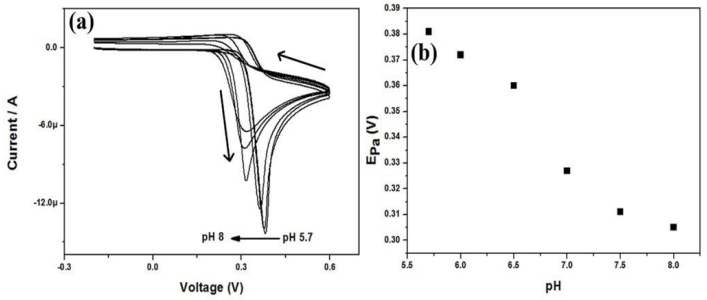

Fig. 16 (a) Cyclic voltammogram of 2mM UA at different pH of PBS buffer solutions at 100mVs^{-1} (b) Plot of anodic peak current vs. different pH from values 5.7 to 8

4. CONCLUSION

The nanostructured duplex stainless steel powder was prepared by using DDPM and studied the morphology of the powder using SEM and HRTEM. Duplex stainless steel show both austenite and ferrite phases; which were indexed by using XRD and SAED ring pattern. BET surface area measurement shows the maximum surface area after milling due to the nano sized particles. DMCPE exhibit strong electro catalytic property towards the oxidation of DA, AA and UA. The 4mg

International Journal of Scientific & Engineering Research, Volume 6, Issue 9, September-2015
ISSN 2229-5518

concentration of duplex stainless steel modified carbon paste electrode show maximum current sensitivity. High selectivity, easy preparation and high sensitivity of the voltammetric response made DMCPE a very useful sensor in determining DA, AA and UA. DMCPE can be used as sensor in medical field for the diagnosis of DA, AA and UA deficiency diseases. Almost all the electrode reactions at the above bioactive compounds are adsorption controlled reactions.

ACKNOWLEDGMENT

Financial support for this work from the Council of Scientific & Industrial Research (CSIR), India (Grant No. 22/561/11/EMR II Dated 11.04.2011) is gratefully acknowledged.

REFERENCES

[1] B.N. Chandrashekar, B.E. Kumara Swamy, M. Pandurangachar, T.V. Sathisha, B.S. Sherigara, "Electropolymerisation of l-arginine at carbon paste electrode and its application to the detection of dopamine, ascorbic and uric acid", *Colloid Surface B.* Vol. 88, pp. 413–418, 2011.

[2] S. Marceglia, G. Foffani, A. Bianchi, G. Baselli, F. Tamma, M. Egidi, A. Priori, "Dopamine dependent non-linear correlation between subthalamic rhythms in Parkinson's disease", *J. Physiol.* Vol. 571, pp. 579–591, 2006.

[3] N. Kemppainen, P. Marjamaki, M. Roytta, J.O. Rinne, "Different pattern of reduction of striatal dopamine reuptake sites in Alzheimer's disease and ageing", *J. Neural Transm.* Vol. 108, pp. 827–836, 2001.

[4] L. Schwieler, G. Engberg, S. Erhardt, "Clozapine modulates midbrain dopamine neuron firing via interaction with the NMDA receptor complex", *Synapse.* Vol. 52, pp. 114–122, 2004.

[5] B.N. Chandrashekar, B.E. Kumara Swamy, M. Pandurangachar, S. Sharath Shankar, Ongera Gilbert, J.G. Manjunatha, B.S. Sherigara, "Electrochemical Oxidation of Dopamine at Polyethylene glycol Modified Carbon Paste Electrode: A Cyclic Voltammetric Study", *Int. J. Electrochem. Sci.* Vol. 5, pp. 578–592, 2010.

[6] J.G. Manjunatha, B.E. Kumara Swamy, G.P. Mamatha, Ongera Gilbert, B.N. Chandrashekar, B.S. Sherigara, "Electrochemical studies of dopamine and epinephrine at a poly (tannic acid) modified carbon paste electrode: a cyclic voltammetric study", *Int. J. Electrochem. Sci*. Vol. 5, pp. 1236–1245, 2010.

[7] K.C. Lin, P.C. Yeh, S.M. Chen, "Electrochemical determination of ascorbic acid using poly (xanthurenic acid) and multi-walled carbon nanotubes", *Int. J. Electrochem. Sci.* Vol. 7, pp. 12752–12763, 2012.

[8] G. Hu, Y. Guo, Q. Xue, S. Shao, "A highly selective amperometric sensor for ascorbic acid based on mesopore-rich active carbon-modified pyrolytic graphite electrode", *Electrochim. Acta.* Vol. 55, pp. 2799–2804, 2010.

[9] The Riordan IVC Protocol for Adjunctive Cancer Care: Intravenous ascorbate as a chemotherapeutic and biological response modifying agent, Riordan Clinic Research Institute. February, pp. 1–21, 2013.

[10] A.B. Florou, M.I. Prodromidis, M.I. Karayannis, S.M. Tzouwara-Karayanni, "Flow electrochemical determination of ascorbic acid in real samples using a glassy carbon electrode modified with a cellulose acetate film bearing 2,6-dichlorophenolindophenol", *Anal. Chimica. Acta.* Vol. 409, pp. 113–121, 2000.

[11] M.S.U. Ali, N. H. Alvi, Z. Ibupoto, O. Nur, M. Willander, B. Danielsson, "Selective potentiometric determination of uric acid with uricase immobilized on ZnO nanowires", *Sensor Actuat B Chem.* Vol. 152, pp. 241–247, 2011.

[12] R. Shashanka, B.E. Kumara Swamy, S. Reddy, D. Chaira, "Synthesis of Silver Nanoparticles and their Applications", *Anal. Bioanal. Electrochem.* Vol. 5, pp. 455–466, 2013.

[13] R. Shashanka, D. Chaira, "Phase transformation and microstructure study of nano structured austenitic and ferritic stainless steel powders prepared by planetary milling", *Powder Technol.* Vol. 259, pp. 125–136, 2014.

[14] R. Shashanka, D. Chaira, "Development of nano-structured duplex and ferritic stainless steels by pulverisette planetary milling followed by pressureless sintering", *Mater Charact.* Vol. 99, pp. 220–229, 2015.

[15] R. Shashanka, D. Chaira, "Optimization of milling parameters for the synthesis of nano-structured duplex and ferritic stainless steel powders by high energy planetary milling", *Powder Technol.* Vol. 278, pp. 35–45, 2015.

[16] B.D. Cullity, S.R. Stock, Elements of X-Ray Diffraction, Pearson, 2003. (Paperback, ISBN-13: 9780131788183).

[17] S. Brunauer, P.H. Emmett, E.J. Teller, "Adsorption of gases in multimolecular layers", *J. Am. Chem. Soc.* Vol. 60, pp. 309–319, 1938.

[18] T. Khalil, F. Abou El-Nour, B. El-Gammal, A.R. Boccaccini, "Determination of surface area and porosity of sol–gel derived ceramic powders in the system TiO_2–SiO_2–Al_2O_3", *Powder Technol.* Vol. 114, pp. 106–111. 2001.

[19] S.J. Gregg, K.S. Sing, "Adsorption, Surface Area and Porosity", Academic Press, London, 1982.

[20] J.G. Manjunatha, B.E. Kumara Swamy, G.P. Mamatha, Ongera Gilbert, M.T. Shreenivas, B.S. Sherigara, "Electrocatalytic Response of Dopamine at Mannitol and Triton X-100 Modified Carbon Paste Electrode: A Cyclic Voltammetric Study", *Int. J. Electrochem. Sci.* Vol. 4, pp. 1706–1718, 2009.

[21] J.G. Manjunatha, B.E. Kumara Swamy, R. Deepa, V. Krishna, G.P. Mamatha, Umesh Chandra, S. Sharath Shankar, B.S. Sherigara, "Electrochemical studies of Dopamine at Eperisone and Cetyl Trimethyl Ammonium Bromide Surfactant modified Carbon paste electrode: A Cyclic Voltammetric Study", *Int. J. Electrochem. Sci.* Vol. 4, pp. 662–671, 2009.

[22] R. Shashanka, D. Chaira, B.E. Kumara Swamy, "Electrocatalytic Response of Duplex and Yittria Dispersed Duplex Stainless Steel Modified Carbon Paste Electrode in Detecting Folic Acid Using Cyclic Voltammetry", *Int. J. Electrochem. Sci.* Vol. 10, pp. 5586 – 5598, 2015.

[23] S. Mahshid, C. Li, S.S. Mahshid, M. Askari, A. Dolati, L. Yang, S. Luoa, Q. Cai, "Sensitive determination of dopamine in the presence of uric acid and ascorbic acid using TiO2 nanotubes modified with Pd, Pt and Au nanoparticles", *Analyst.* Vol. 136, pp. 2322–2329, 2011.

[24] B.J. Venton, M. Wightman, "Psychoanalytical electrochemistry: dopamine and behavior", *Anal. Chem.* Vol. 75, pp. 414A–421A, 2003.

[25] F. Martinello, E.L. Da Silva, "Ascorbic acid interference in the measurement of serum biochemical parameters: in vivo and in vitro studies", *Clin. Biochem.* Vol. 39, pp. 396–403, 2006.

[26] P.S. Cahill, Q.D. Walker, J.M. Finnegan, G.E. Mickelson, E.R. Travis, R.M. Wightman, "Microelectrodes for the measurement of catecholamines in biological systems", *Anal. Chem.* Vol. 68, pp. 3180–3186, 1996.

[27] O. Gilbert, B.E.K. Swamy, U. Chandra, B.S. Sherigara, "Simultaneous detection of dopamine and ascorbic acid using polyglycine modified carbon paste electrode: A cyclic voltammetric study", *J. Electroanal. Chem.* Vol. 636, pp. 80–85, 2009.